Atypical disseminated intravascular coagulopathy during bubonic plague

Guillain Mikaty, Christian Demeure, Sofia Filali, Javier Pizarro-Cerda, Pierre Goossens, Elisabeth Carniel

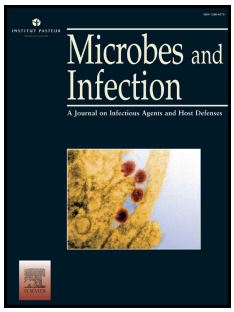

Atypical disseminated intravascular coagulopathy during bubonic plague

Guillain Mikaty, Christian Demeure, Sofia Filali, Javier Pizarro-Cerda, Pierre Goossens, Elisabeth Carniel

PII: S1286-4579(22)00133-2

DOI: https://doi.org/10.1016/j.micinf.2022.105063

Reference: MICINF 105063

To appear in: *Microbes and Infection*

Received Date: 30 May 2022

Revised Date: 6 October 2022

Accepted Date: 19 October 2022

Please cite this article as: G. Mikaty, C. Demeure, S. Filali, J. Pizarro-Cerda, P. Goossens, E. Carniel, Atypical disseminated intravascular coagulopathy during bubonic plague, *Microbes and Infection*, https://doi.org/10.1016/j.micinf.2022.105063.

Atypical disseminated intravascular coagulopathy during bubonic plague

Guillain Mikaty[ab*], Christian Demeure[a], Sofia Filali[a], Javier Pizarro-Cerda[a], Pierre Goossens[b§], Elisabeth Carniel[a§]

a. Institut Pasteur, Université Paris Cité, Yersinia Research Unit, F-75015 Paris, France.

b. Institut Pasteur, Université Paris Cité, Unité de Pathogénie des Toxi-Infections Bactériennes, F-75015 Paris, France.

*** Corresponding author**

Guillain Mikaty ;

Yersinia Research Unit

Institut Pasteur

28 rue du Dr. Roux

75724 Paris Cedex 15

France

Phone: +33 1 45 68 87 58

Fax: +33 1 40 61 38 07

E-mail: guillain.mikaty@pasteur.fr

[§]Co-senior authors

Pierre Goossens and Elisabeth Carniel

Number of text pages: 13 (including Abstract)

Number of Figures: 3

Number of Tables: 1

Running title:

Coagulopathy during plague and anthrax

Funding statement:

GM received grants from the CEA (NRBC projetc #17.1) and from ANR and DGA (ANR-12-ASTR-0024).

Competing Interest:

The author(s) declare no competing interests.

Author contributions

GM, EC and PG designed the project; GM, CD and SF performed all experiments; GM and EC wrote the main manuscript text. All authors reviewed the manuscript.

Footnote:

Guillain Mikaty's current affiliation: Environment and Infectious Risks research and expertise Unit, Laboratory for urgent response to biological threats (ERI-CIBU), Institut Pasteur, Paris, France.

Abstract (Word count: <200)

Powerful pathogens such as *Bacillus anthracis* and *Yersinia pestis* cause severe hemorrhagic syndromes that have previously been attributed to a Disseminated Intravascular Coagulopathy (DIC). However, the data attesting this statement are missing or contradictory. This study aimed at determining whether a DIC do occur at the late stages of plague and anthrax. Using the mouse models of cutaneous anthrax and bubonic plague, we observed that most *B. anthracis*-infected animals exhibited increased partial thromboplastin time (aPTT) and prothrombin time (PT), along with a dynamic consumption of fibrinogen, matching the characteristics of an overt DIC. In contrast, only heavily *Y. pestis*-infected mice displayed increased aPTT, but little fibrinogen consumption and no increase of PT were observed in most infected animals, even at late stages of infection. Therefore, the coagulopathy that develops during anthrax is compatible with a classical DIC, while *Y. pestis*-infected mice do not present with typical parameters. This suggests that the mechanism involved in the hemorrhages observed during bubonic plague is not a classical DIC, and that the coagulopathy exhibits a specific, atypical pattern. It is then important to understand how these hemorrhages are triggered.

Keyword: DIC; Yersinia pestis; Bacillus anthracis

1. Introduction

Hemorrhages are the mark of powerful and deadly pathogens, and they often participate to the severity and morbidity of infectious diseases. Only a few bacteria are capable of inducing systemic bleedings. Both the Gram-negative *Yersinia pestis* and the Gram-positive *Bacillus anthracis*, which are among the most potent bacterial pathogens, may cause severe hemorrhagic syndromes.

Bubonic plague is the most common clinical presentation of *Y. pestis* infection in humans and animals. It occurs after a fleabite and is characterized by the formation of a swelling lymph node (bubo) draining the site of injection. From the bubo, *Y. pestis* reaches the bloodstream and disseminates. Hemorrhages in all tissues have been commonly observed during post-mortem pathological examinations of human victims who died of bubonic plague [1]. Comparable hemorrhages and external bleeding have also been described in naturally infected animals [2] and in experimental animal models [3].

Cutaneous anthrax, the most frequent form of *B. anthracis* infection in humans, also leads to the multiplication of *B. anthracis* in the draining lymph node [4]. The bacilli then enter the bloodstream, causing blood vessel leakage and hemorrhages in human victims and animal models [5-7]. At the final stage of the disease, patients harbor dark and non-coagulable blood known as “anthrax blood” [8]. It has been shown that the two well-characterized toxins of *B. anthacis*, the edema toxin (ET) and the lethal toxins (LT), can induce hemorrhages by themselves [9-10]. However, recent scientific investigations have shown that the bacillus can induce bleeding regardless of the action of the two toxins [11-12].

The hemorrhages observed during anthrax and plague have often been described the consequence of a disseminated intravascular coagulopathy (DIC) [11, 13-15]. However, bacterial-induced DIC is usually characterized by a generalized internal organs failure due to disseminated fibrin clots in vessels [16], rather than bleedings that occur in only ~15% of cases

[17]. Additionally, specific data supporting this DIC hypothesis are scarce, partly missing or contradictory. For infection by *Y. pestis*, no fibrinogen decrease has been reported, and prothrombin time was not measured or was not prolonged. DIC is a pathological process characterized by the over-activation of the blood coagulation cascade (Fig.1). The transient formation of blood clots in vessels is followed by their fibrinolytic disruption and by a complete consumption of key coagulation factors such as fibrinogen, prothrombin, factor V and platelets, ultimately leading to multiple organs failure (due to numerous fibrin clots) and/or severe bleeding (due to the exhaustion of coagulation capacities and the absence of repair of blood vessels). In addition, the release of bacterial inflammatory factors, such as LPS or peptidoglycans during severe and systemic bacterial infections causes a generalized activation of clotting factors in the blood [16]. According to the classical view, here called *the canonical pathway*, the initiation of the DIC depends on the release of the Tissue Factor (TF), generally through the trauma of vascular or circulating cells, leading to the activation of the extrinsic pathway of coagulation [18-19]. The extrinsic pathway eventually provokes the activation of platelets and the formation of disseminated fibrin clots in the microvessels (Fig.1). Clots of fibrin are quickly degraded by fibrinolysis following the activation of plasminogen into plasmin. This initial pathway is rapidly amplified by the activation of the intrinsic pathway, notably through the inflammation that usually accompanies the process.

Fig.1

DIC may be induced by different diseases and multiple mechanisms, hence the biological parameters used to define the phenomenon are those common to all processes. The biological signs used to define a DIC include: an elongation of the prothrombin time (PT), measuring the extrinsic pathway of coagulation (Fig.1); an elongation of the activated partial thromboplastin time (aPTT), measuring the intrinsic pathway; a dramatic decrease of plasmatic fibrinogen levels, due to the formation of fibrin clots; a drop of platelet levels; and an increase of products

of fibrin degradation (FDP), following fibrinolysis. These parameters reflect the underlying consumption of clotting factors in both the extrinsic (measured with PT) and intrinsic (measured with aPTT) pathways of coagulation and fibrinolysis. However, the whole process is very dynamic and biological parameters used to measure the phenomenon are not always decisive, especially early in the process, when the DIC is compensated. Nonetheless, once the coagulation factors are consumed, the coagulopathy is said *overt DIC*, or *decompensated DIC*, and all biological parameters show clear defects in the coagulation of both pathways.

The conjunction of severe bacterial infection and disseminated hemorrhages dramatically increases the risk of fatal outcomes. Since therapeutic strategies could be used to improve the vital prognosis of patients with DIC, as previously proposed for plague [14], it is of key importance to revisit existing data and determine whether a true DIC occurs at the late stages of plague and anthrax. Here, we tested the hemostatic parameters of mice infected either with *B. anthracis* or *Y. pestis* to evaluate whether DIC actually occurs during the pathogenesis of these two bacteria and could account for the hemorrhages observed. We found that *B. anthracis* induces a coagulopathy resembling an overt DIC while *Y. pestis* displays a more complex pattern of coagulation defects. We propose that each of these pathogens induces a specific DIC through different mechanisms and that *Y. pestis* mechanisms do not correspond to the canonical pathway as described in the literature.

2. Materials and Methods

2.1.Bacteria and growth conditions

The *Y. pestis* strains used in this study were the fully virulent wild type strain CO92 [20] and the plasmid cured *Y. pestis* ΔpPla strain [21]. Bacteria were cultured at 28°C for 36h on Luria Bertani agar plates supplemented with 0.002% (w/v) hemin (LBH) and were suspended in phosphate buffered saline (PBS). The concentrations of the resulting suspensions were estimated by measuring the optical density at 600 nm and were confirmed by cfu count on LBH.

The *Bacillus anthracis* strain used was the encapsulated non-toxinogenic Δ*pagA* 9602P strain. Spores were diluted in PBS and the final concentrations were confirmed by serial plating on Brain Heart Infusion (BHI) agar plates.

2.2.Animal experiments

Six-week-old OF1 female mice (Charles River Laboratory) were housed in the Institut Pasteur biosafety level 3 animal facility accredited by the French Ministry of Agriculture (accreditation B 75 15–01), in compliance with French and European regulations on care and protection of Laboratory Animals (EC Directive 86/609, French Law 2001–486 issued on June 6, 2001). Mouse infections were carried out following approved protocols by the Institut Pasteur ethic comity for animal experimentation (CETEA Institut Pasteur, "Comité d'Ethique en Expérimentation Animale" registered by the French Ministry of Education and Research (MESR) under the number 89) ; approved protocols CETEA 2014-0025/MESR 08223 for *Y. pestis* and CETEA 2013-0088/MESR 01168.01 for *B. anthracis*. Lipopolysaccharide (LPS) from *E. coli* 011:B4 (Interchim) at a dose of 7.5, 15 or 35 mg/kg was administered intraperitoneally to groups of 10 mice 16h before hemostasis analyses. *Y. pestis* CO92 ($1.5x10^3$ bacilli), *Y. pestis* ΔpPla ($2x10^6$ bacilli) or the encapsulated non-toxinogenic Δ*pagA* 9602P *B. anthracis* strain (10^6 spores) were injected subcutaneously to groups of 10 mice 24h-36h before hemostasis analyses. For *Y. pestis*, the experiment was repeated in order to obtain enough surviving animals to interpret the results, thus 14 additional mice were challenged to compensate for dead individuals. Control mice received subcutaneously 100 µl of PBS. The apparent state of sickness of the animals was scored. The mice were sacrificed and their spleen and blood were collected. Bacterial loads were determined by plating blood samples and spleen homogenates on LBH (*Y. pestis*) or BHI (*B. anthracis*) plates. These loads were quantified precisely for *Y. pestis,* while only thresholds were determined for *B. anthracis.*

In a second series of experiments, 10^2 *Y. pestis* bacilli were injected subcutaneously to

groups of five to ten mice. The mice were sacrificed every 24h for 5 days and their spleen and blood were collected. The bacterial loads in these samples were quantified as described above.

2.3.Hemostasis analyses

Hemostasis tests were performed on blood samples containing 0.0109 M citrate final, using the kits STA-Fibri-Prest® Automate, and STA®-Liquid Fib, STA-Neoplastine® Cl Plus, D-Di Test and STA-PTT Automate from Diagnostica Stago. The blood volumes were divided by half (50 ul) compared to usual protocols after validation of the precision and reproducibility with a STA-Unicalibrator. For *Y. pestis* and LPS, the hemostasis measurements were performed in a biosafety level 3 laboratory, and time to form a fibrin clot was determined visually in glass tubes (estimated precision of 0.5s). For *B. anthracis,* the coagulation time was determined using the STart® 4 machine from Diagnostica Stago (estimated precision of 0.1s). The comparability of the results obtained with the two methods was confirmed on samples from mice that received PBS or LPS.

2.4.Statistical analyses

All data were compared with the non-parametric test of Mann-Whitney using the Prism software version 6.07 (Graph Pad Software). Significance were set at $P<0.05$. Value of aPTT were tested with a two-tailed test while PT were tested with a one-tailed test. * $P<0.05$; ** $P<0.001$.

3. Results

To evaluate hemostasis alterations during bubonic plague and cutaneous anthrax, we first determined normal values for blood aPTT, PT and fibrinogen in our animal model, using a group of 10 animals that had received PBS subcutaneously (Table 1 and Fig.2A). As a positive control for DIC, we used the mouse experimental model of LPS injection [22]. As expected, LPS-inoculated mice exhibited clinical symptoms related to the amount of LPS injected (Table 1). Their PT and aPTT increased with the concentrations of LPS injected (Table 1 and Fig.2B).

Both aPTT and PT of the LPS-injected mice were significantly different from the PBS control mice using the Mann-Whitney *U* test (aPTT: **P<0.0001, PT: **P=0.0003). The fibrinogen blood concentrations were increased at the lowest dose of LPS and decreased at the highest dose (Table 1), indicative of the dynamic activation and subsequent consumption of this factor [22]. The extension of aPTT and PT is the demonstration of a global coagulation defect and is commonly used in the first-line diagnosis of DIC. For some of the mice, we tested the presence of FDPs (fibrin degradation products due to fibrinolysis) using a non-quantitative agglutination method. Characteristic FDP agglutination was observable with LPS-injected animals confirming the intense fibrinolysis accompanying the DIC. Fibrinogen consumption, which is representative of the intense formation of fibrin clots prior to the fibrinolysis process, also confirmed the diagnostic.

Table 1

Fig.2

Mice infected with *B. anthracis* often had high bacterial loads in spleen ($\geq 10^7$ cfu) and blood ($\geq 10^5$ cfu/ml), but their clinical symptoms did not correlate with the intensity of the bacteremia (Table 1 and Fig.2C). Most infected animals (7/10) had prolonged PT (13.8s to 20s) and aPTT (69s to >100s), whereas one third (3/10) of them presented no defect in aPPT or PT in spite of patent sickness symptoms and the presence of bacteria in their spleen and blood. The aPTT and PT of the *B. anthracis*-challenged mice were significantly different from the PBS control mice (aPTT: **P=0.0001, PT: *P=0.0017) but were not distinguishable from the group of LPS injected mice (aPTT: P=0.2461, PT: P=0.3349), indicating comparable coagulation processes. Fibrinogen levels displayed a large range of values (from 1.82 to 4.04 mg/ml) (Table 1) which probably reflected different stages of the activation/consumption process. The blood taken from these mice looked dark, fitting the description of “anthrax blood". Overall, although there was no direct correlation between the clinical status and the hemostatic disorders measured, the

increased PT and aPPT observed in most *B. anthracis*-infected mice fitted with the definition of a canonic DIC. Furthermore, our results based on the use of a non-toxinogenic Δ*pagA* strain confirmed recent findings that LT and ET toxins are not necessary to induce such coagulation defect [11-12]. These results also suggested that although the DIC was concomitant with disease progression, it was not the main factor causing the symptoms.

Of 10 mice infected with *Y. pestis*, four mice were already dead at 24h because of the high bacterial inoculum ($1.5x10^3$ cfu) used, and therefore could not be included in the analysis. We repeated the experiment and pooled the results in order to obtain enough animals to interpret the outcomes. Three of the surviving mice presented no bacteremia and had a moderate bacterial load in the spleen ($<10^6$ cfu), together with mild signs of infection (Table 1). PT and aPTT, parameters were normal and the elevated fibrinogen concentration was in line with an early stage of infection. Five mice presented with a more advanced stage of infection, with bacteremia (10^3 to 5.10^4 cfu/ml) along with moderate to strong symptoms. They had a normal PT, an elevated aPTT but within the normal limit (48-50), and a higher fibrinogen concentration than the three previous mice. Four mice had major signs of infection that fitted with high bacterial loads in the spleen ($>10^6$ cfu) and the presence of bacteria in the blood (Table 1 and Fig.2D). Three of them were moribund. The four mice displayed an elevated aPPT (52s to 85s), although not as high as that observed for *B. anthracis*-infected mice. Strikingly, their PT were within normal values (11-12.5). There were signs of fibrinogen consumption, as evidenced by a level of this factor higher than in the control mice, but lower than in the five previous less sick mice (4.5-5 mg/ml compared to 4.9-6.35 mg/ml). The three last mice were also moribund with high levels of bacteria in their blood and spleen, and displayed *overt DIC*: elongated PT and aPTT along with low fibrinogen level for one mouse. The PT and aPTT in the group of *Y. pestis*-infected mice were significantly different from the PBS control mice (PT: **P=0.0084; aPTT: **P=0.00008) but not from the LPS challenged mice (PT: P=0.1238; aPTT: P=0.9806).

Some of the *Y. pestis*-infected mice presenting with coagulation defect were tested and showed the presence of FDP characteristic of intense fibrinolysis. Interestingly, *Y. pestis* presented with a coagulation defect different from that of *B. anthracis*: coagulation factors of the intrinsic pathway, measured with the aPTT, were consumed before those of the extrinsic pathway, showing a pattern that did not correspond to the canonical pathway of activation of DIC.

Y. pestis carries a plasmid called pPla, which encodes a plasminogen activator known to play an important role in the pathogenicity of the bacterium. Because of the central function of plasminogen activation as an activator of fibrinolysis we tested a strain of *Y. pestis* cured of pPla. We adjusted the inoculum of the ΔpPla strain to mimic the disease progression of the parental strain [21] and measured the hemostatic parameters of *Y. pestis*ΔpPla-infected mice. All mice presented with moderate to high loads of bacteria in the spleen (10^5 to 10^9 cfu) and bacteremia in blood, probably due to the high initial inoculum. Six out of ten mice had moderate to severe symptoms, not associated with any coagulation defect. Two mice presented with severe symptoms associated with elevated aPTT (80s and 98s) but normal PT (10s and 11s). The last two mice died before the analysis. The ΔpPla strain reproduced the same hemostatic pattern as the parental strain and showed a non-canonical activation of the DIC (Table 1 and Fig.2E).

Fig.3

To further understand the initiation of the DIC in *Y. pestis*-infected mice, we repeated the experiment with a lower bacterial inoculum and followed the kinetics of bacterial multiplication in spleen and blood, along with aPPT and PT values. Because some animals were already moribund on day 4 (D4), introducing a bias of selection at late stages of infection, the data from D4 and D5 were pooled. We observed an increase of the bacterial load in the spleen from D1 to D4/5 (Fig.3A) and a bacteremia which started on D3 and affected the majority of animals on D4/5 (Fig.3B). For most animals, the aPTT values remained within the normal limits until D3

but they went past the threshold on D4/5 in 60% of infected mice (Fig.3C). The distribution of values of aPTT for the *Y.pestis*-infected mice was significantly different from those of PBS-challenged mice (*P=0.0072) but not from LPS (P=0.42) observed in Table 1. The animals with an increased aPTT were bacteremic and had high bacterial loads in their spleen. However, some heavily infected and bacteremic mice still had a normal aPTT. With the exception of two mice on D4/5, the PT remained within the normal range or at the threshold, in the majority of mice (Fig.3D), even when their aPTT was prolonged, and despite the fact that they had bacteremia and high bacterial loads in their spleen. The distribution of values of PT for these mice was significantly different from those of PBS-challenged mice (*P=0.0038) and also from LPS-challenged mice (*P=0.028) observed in Table 1, demonstrating a unique pattern for the coagulopathy of these animals. These results describe a kinetic of elongation of the coagulation time that starts with the intrinsic pathway before impairing the extrinsic pathway. In agreement, mice were moribund and would have probably died before any defect in the extrinsic pathway would be measurable. These data thus confirm that most *Y. pestis*-infected mice present with a compensated DIC not initiated through the extrinsic pathways, as suggested by the canonical view, and our observation that mice can die from plague before the installation of an *overt DIC*.

4. Discussion

In this study, we confirm that hemostasis alterations that take place during cutaneous anthrax are consistent with an overt DIC, as previously proposed [10-12], and are independent of the production of both LT and ET toxins. In contrast, we show that *Y. pestis* induces an atypical coagulopathy that does not match the canonical DIC described in the literature.

The analysis of the hemostatic status of human bubonic plague patients with clinical signs of purpura in the early 1970s indicated prolonged aPTT, low platelet counts, and positive ethanol gelation tests (which detect circulating fibrin monomers) [14]. In the mouse experimental model of bubonic plague, extended clotting times and aPTT were also reported,

along with a decreased platelet numbers [15]. The alteration of these hemostasis factors was attributed to a DIC although some data were lacking or were sometimes contradictory, such as no fibrinogen decrease, PT not measured or not prolonged. This shortcut was probably accepted because of similar but more comprehensive studies on the pneumonic model of plague [13]. However, the physiopathology of pneumonic plague is different from that of the bubonic form, particularly with regard to the inflammatory process [23]. During pneumonic plague in *Macaca mulatta*, prolonged PT and aPTT were observed, suggesting an actual overt DIC. This coagulopathy occurred along with an increased inflammatory response after 36 hours [23]. Here we show that at the pre-mortem phase of bubonic plague, *Y. pestis* induces a coagulopathy characterized by a prolonged aPTT, but with normal PT values and only a moderate consumption of fibrinogen, as compared to LPS-induced DIC or during anthrax. The fact that a ΔpPla strain of *Y. pestis*, which lacks the plague plasminogen activator, displayed the same type of coagulopathy profile as the wild type strain indicates that fibrinolysis is not important in the initiation of this particular hemostatic disorder.

DIC diagnosis is defined by the prolongation of coagulation time, demonstrating a global coagulation defect confirmed by measuring fibrinolysis. According to the canonical view of DIC, the disseminated coagulation starts with the release of TF, induced through different mechanisms, and prompting the initiation of the extrinsic pathway (measured with PT). The deregulated phenomenon is amplified through the secondary activation of the intrinsic pathway (measured by aPTT) [18]. Various studies have questioned the value of PT, aPTT and fibrinogen to diagnose DIC [24-25], in particular considering that DIC is a dynamic process and that these tests can stay within normal value early in the process, while the DIC is still compensated. Additionally, this canonical view of DIC has been challenged and scientists proposed more recently that the initiation of DIC could be multifactorial and varies depending on the underlying cause [17, 26, 27]. In the case of bacterial-induced sepsis, it is thought that

the inflammatory process, notably due to LPS release from Gram-negative bacteria, initiates TF activation of the intrinsic pathway, usually provoking a DIC characterized by a generalized internal organ failure due to numerous blood clots [19]. As a corollary, bleeding consecutive to a DIC is rare during bacterial infections and occurs in only ~15% of cases [17]. Here we tested two bacterial pathogens commonly causing bleeding, and we show that their mechanism of DIC induction is different from each other. While *B. anthracis* provokes rapidly an uncompensated DIC with classic hemostatic parameters, *Y. pestis* on the other hand, induces a coagulation defect that is characterized by an initial consumption of factors of the intrinsic pathway before a more global coagulation defect. In a recent work, we have shown that the interaction between *Y. pestis* and the blood vessels is very brutal [28]. The plague bacillus is capable of degrading blood vessels within the organs before reaching the circulating blood. Then, the bacilli circulating in the bloodstream seem to be capable to cross back the endothelial vascular barrier by opening tight junction to reach secondary organs [28]. These phenomena happen as early as 48h post-infection, and local bleedings are observable within the infected organs at a time when no coagulation defects are measured. We thus propose that the interaction of *Y. pestis* with blood vessels, in particular the opening of tight junctions, might specifically trigger the intrinsic pathway through contact activation with the subendothelial extracellular matrix. Following this initiation of disseminated coagulation at the sites of bacterial crossing of the blood barrier, the whole coagulation cascade would be activated, sometimes leading to an overt DIC, when the victim did not die from the infection before.

Of note, we have observed for both *B. anthracis* and *Y. pestis*, that the state of the DIC is not directly correlated with the fatal outcome. Some moribund *B. anthracis*-infected animals had normal coagulation parameters, and inversely, animals looking fine could display an advanced DIC. Similarly, some moribund *Y. pestis*-infected mice presented a compensated DIC with normal PT parameters. In both cases, the bacterial invasion of all organs was likely the cause

of the host death, while the coagulation defect only aggravated factor the disease outcome. Thus, coagulation parameters might not be a good indicator of the disease progression for these two pathogens. Since the atypical DIC unveiled here results from a mechanism specific to *Y. pestis*, elucidating it might open ways to block it, and therefore improve the outcome of plague patients. Additionally, the symptomatic treatment of the coagulation defect might have importance to mitigate consequences for survivors, such as the loss of extremities (fingers, toes, nose, etc.) due to gangrene.

Altogether our data thus demonstrate that hemorrhagic bacterial pathogens induce bleeding in their host by different and probably specific mechanisms, and that *Y. pestis* induces a specific coagulation pattern different from the canonical view of the DIC. We believe this work supports the recent hypotheses that DIC cannot be limited to the canonical view and is actually a multifactorial syndrome with specific alterations of biological parameters depending on the initiating cause.

Acknowledgments

The authors would like to thank Thomas Labadie for his help with the statistical analyses. GM received grants from the CEA (NRBC project #17.1) and ANR-DGA (ANR-12-ASTR-0024).

References

[1]. Flexner S. The pathology of bubonic plague. Am J Med Sci. 1901;396-416.

[2]. Wong D, Wild MA, Walburger MA, Higgins CL, Callahan M, Czarnecki LA, et al. Primary Pneumonic Plague Contracted from a Mountain Lion Carcass. Clinical Infectious Diseases. août 2009;49(3):e33-8.

[3]. Guinet F, Avé P, Jones L, Huerre M, Carniel E. Defective Innate Cell Response and Lymph Node Infiltration Specify Yersinia pestis Infection. Nielsen K, éditeur. PLoS ONE. 27 févr 2008;3(2):e1688.

[4]. Goossens PL. Animal models of human anthrax: the Quest for the Holy Grail. Mol Aspects Med. déc 2009;30(6):467-80.

[5]. Abramova FA, Grinberg LM, Yampolskaya OV, Walker DH. Pathology of inhalational anthrax in 42 cases from the Sverdlovsk outbreak of 1979. Proc Natl Acad Sci U S A. 15 mars 1993;90(6):2291 4.

[6]. Guarner J, Jernigan JA, Shieh W-J, Tatti K, Flannagan LM, Stephens DS, et al. Pathology and pathogenesis of bioterrorism-related inhalational anthrax. Am J Pathol. août 2003;163(2):701-9.

[7]. Stearns-Kurosawa DJ, Lupu F, Taylor FB, Kinasewitz G, Kurosawa S. Sepsis and pathophysiology of anthrax in a nonhuman primate model. Am J Pathol. août 2006;169(2):433-44.

[8]. World Health Organization, Nations F and AO of the U, Health WO for A. Anthrax in humans and animals [Internet]. World Health Organization; 2008 [cited 23 mars 2022]. 208 p. available on: https://apps.who.int/iris/handle/10665/97503

[9]. Maddugoda MP, Stefani C, Gonzalez-Rodriguez D, Saarikangas J, Torrino S, Janel S, et al. cAMP signaling by anthrax edema toxin induces transendothelial cell tunnels, which

are resealed by MIM via Arp2/3-driven actin polymerization. Cell Host Microbe. 17 nov 2011;10(5):464-74.

[10]. Rolando M, Stefani C, Flatau G, Auberger P, Mettouchi A, Mhlanga M, et al. Transcriptome dysregulation by anthrax lethal toxin plays a key role in induction of human endothelial cell cytotoxicity. Cell Microbiol. juill 2010;12(7):891-905.

[11]. Qiu P, Li Y, Shiloach J, Cui X, Sun J, Trinh L, et al. Bacillus anthracis cell wall peptidoglycan but not lethal or edema toxins produces changes consistent with disseminated intravascular coagulation in a rat model. J Infect Dis. sept 2013;208(6):978-89.

[12]. Remy KE, Qiu P, Li Y, Cui X, Eichacker PQ. B. anthracis associated cardiovascular dysfunction and shock: the potential contribution of both non-toxin and toxin components. BMC Medicine [Internet]. déc 2013 [cited 26 mars 2019];11(1). Available on: http://bmcmedicine.biomedcentral.com/articles/10.1186/1741-7015-11-217

[13]. Finegold MJ, Petery JJ, Berendt RF, Adams HR: Studies on the pathogenesis of plague. Blood coagulation and tissue responses of *Macaca mulatta* following exposure to aerosols of *Pasteurella pestis*. Am J Pathol 1968, 53:99-114

[14]. Butler T: A clinical study of bubonic plague. Observations of the 1970 Vietnam epidemic with emphasis on coagulation studies, skin histology and electrocardiograms. Am J Med 1972, 53:268-276

[15]. Kiseleva I. Observations on the mechanism of the hemorrhages in plague, report 1. State of the factors of blood coagulation in experimental plague. Don State Scientific-Research Antiplague Institute. 1959;Vol XV:97-105.

[16]. Asakura H. Classifying types of disseminated intravascular coagulation: clinical and animal models. J Intensive Care. 2014;2(1):20.

396 [17]. Okajima K, Sakamoto Y, Uchiba M. Heterogeneity in the incidence and clinical
397 manifestations of disseminated intravascular coagulation: a study of 204 cases. Am J
398 Hematol. nov 2000;65(3):215-22.
399 [18]. Papageorgiou C, Jourdi G, Adjambri E, Walborn A, Patel P, Fareed J, et al.
400 Disseminated Intravascular Coagulation: An Update on Pathogenesis, Diagnosis, and
401 Therapeutic Strategies. Clin Appl Thromb Hemost. déc 2018;24(9_suppl):8S-28S.
402 [19]. Levi M, ten Cate H, Bauer KA, van der Poll T, Edgington TS, Büller HR, et al.
403 Inhibition of endotoxin-induced activation of coagulation and fibrinolysis by pentoxifylline
404 or by a monoclonal anti-tissue factor antibody in chimpanzees. J Clin Invest. janv
405 1994;93(1):114-20.
406 [20]. Parkhill J, Wren BW, Thomson NR, Titball RW, Holden MTG, Prentice MB, et al.
407 Genome sequence of Yersinia pestis, the causative agent of plague. Nature. oct
408 2001;413(6855):523-7.
409 [21]. Guinet F, Avé P, Filali S, Huon C, Savin C, Huerre M, et al. Dissociation of Tissue
410 Destruction and Bacterial Expansion during Bubonic Plague. O'Riordan M, éditeur. PLOS
411 Pathogens. 20 oct 2015;11(10):e1005222.
412 [22]. Levi M, Dörffler-Melly J, Reitsma P, Buller H, Florquin S, van der Poll T, et al.
413 Aggravation of endotoxin-induced disseminated intravascular coagulation and cytokine
414 activation in heterozygous protein-C-deficient mice. Blood. 15 juin 2003;101(12):4823-7.
415 [23]. Pechous RD, Sivaraman V, Stasulli NM, Goldman WE. Pneumonic Plague: The
416 Darker Side of Yersinia pestis. Trends Microbiol. mars 2016;24(3):190-7.
417 [24]. Yu M, Nardella A, Pechet L. Screening tests of disseminated intravascular
418 coagulation: guidelines for rapid and specific laboratory diagnosis. Crit Care Med. juin
419 2000;28(6):1777-80.

[25]. Bick RL, Baker WF. Diagnostic efficacy of the D-dimer assay in disseminated intravascular coagulation (DIC). Thromb Res. 15 mars 1992;65(6):785-90.

[26]. Thachil J. The Elusive Diagnosis of Disseminated Intravascular Coagulation: Does a Diagnosis of DIC Exist Anymore? Semin Thromb Hemost. févr 2019;45(1):100-7.

[27]. Drouet L. Il existe non pas une, mais plusieurs CIVD. Sang Thrombose Vaisseaux. 1 mars 2010;22(3):6-19.

[28]. Mikaty G, Coullon H, Fiette L, Pizarro-Cerdá J, Carniel E. The invasive pathogen Yersinia pestis disrupts host blood vasculature to spread and provoke hemorrhages. PLoS Negl Trop Dis. 5 oct 2021;15(10):e0009832.

Table 1. Hemostasis parameters in mice that received PBS (negative control), LPS (positive control for DIC), *B. anthracis* or *Y. pestis*.

Treatment	aPPT (s)	PT (s)	Fibrinogen (mg/ml)	Spleen[a] (cfu/organ)	Blood[a] (cfu/ml)	Clinical status[b]
Control[c]	20-50	9–13	1.9–2.9	NA	NA	0
LPS[d] (mg/kg)						
7.5	46	11	4.53	NA	NA	+
7.5	48.1	11.2	ND	NA	NA	+
7.5	58	13	3.86	NA	NA	+
7.5	61	13	3.59	NA	NA	+
7.5	62	13	3.36	NA	NA	+
15	51	18	2.32	NA	NA	++
15	52.5	17	2.14	NA	NA	++
15	61.1	16	2.32	NA	NA	++
35	64	15.3	<0.88	NA	NA	+++
35	>90	>90	<0.88	NA	NA	+++
B. anthracis[e]						
	35.1	10.4	ND	$\geq 10^7$	$\geq 10^5$	+
	42.4	11.2	2.7	$<10^7$	$\geq 10^7$	++
	41.6	11.4	3.76	ND	ND	++
	69	13.8	1.82	ND	ND	++
	80	15	ND	$\geq 10^7$	$\geq 10^7$	+
	>100	20	4.04	$\geq 10^7$	$\geq 10^5$	+
	>100	16	4.04	$\geq 10^7$	$\geq 10^5$	+++
	100	14.7	2.44	ND	ND	++
	>100	15	2.55	$\geq 10^7$	$\geq 10^5$	++
	>100	15	2.8	$\geq 10^7$	$\geq 10^7$	+++
Y. pestis[f]						
	41	11	4.17	8.2×10^2	0	+
	44	11	4.97	4.5×10^4	0	+
	<30	12	4.17	7.0×10^5	0	+
	42	11.5	4.8	2.0×10^7	5.0×10^4	+++
	48	11	4.9	4.0×10^4	3.5×10^3	++
	49	11.5	6.35	2.6×10^4	5.5×10^3	++
	49	12.5	5.9	1.4×10^4	2.8×10^7	+++

	50	11.5	5.05	$5.3x10^4$	$3.5x10^3$	++
	52	11	4.53	$4.1x10^6$	$3.0x10^3$	+++
	53	12.5	ND	$1.4x10^4$	$7.5x10^3$	++
	57	12.5	4.97	$9.0x10^7$	$1.8x10^5$	+++
	85	12.5	4.53	$2.0x10^6$	$1.5x10^5$	+++
	61	14	ND	$2.0x10^7$	nd	+++
	60	14.5	ND	$5.1x10^4$	$5.0x10^7$	+++
	94	15.5	1.5	$1.0x10^8$	$5.0x10^7$	+++
Y. pestis ΔpPla[g]						
	<30	11	ND	$1x10^2$	$1x10^2$	+
	<30	10	ND	$2.5x10^8$	ND	++
	31	10	ND	$8.5x10^8$	$1x10^6$	++
	38	11	ND	$1.2x10^8$	$8x10^6$	++
	42	10	ND	$2.5x10^5$	$1x10^2$	+++
	46	11	ND	$2x10^6$	$1x10^2$	+++
	80	10	ND	$3x10^6$	$1x10^2$	+++
	98	11	ND	$1.3x10^7$	$1x10^5$	+++

Ordering was based on increasing severity of the parameters and symptoms. Each line corresponds to one mouse.

Abbreviations: aPPT: Activated partial thromboplastin time; PT: Prothrombin time; NA: not applicable; ND: not determined.

[a] Precise bacterial loads for *Y. pestis* and thresholds for *B. anthracis*.

[b] 0: healthy; +: sick (slight shivering and slow movement); ++: very sick (shivering and prostrated but still reactive to stimuli); +++: moribund (shivering, prostrated and irresponsive).

[c] Control mice received PBS subcutaneously and were used to define normal ranges (80% to 120% of normal values ±standard deviation) for hemostasis parameters.

[d] 10 mice received LPS intraperitoneally 16h before blood sampling and were used as positive controls for hemostasis disorders that characterize a DIC.

[e] 10 mice were subcutaneously infected with 10^6 spores of *B. anthracis* Δ*pagA* 9602P 24h prior to blood sampling.

[f] 10 +14 mice were subcutaneously infected with $1.5x10^3$ cfu of *Y. pestis* CO92 24h prior to blood sampling. Six animals died before sampling.

[g] 10 mice were subcutaneously infected with $2x10^6$ *Y. pestis* ΔpPla prior to blood sampling. Two animals died before sampling.

Figure 1

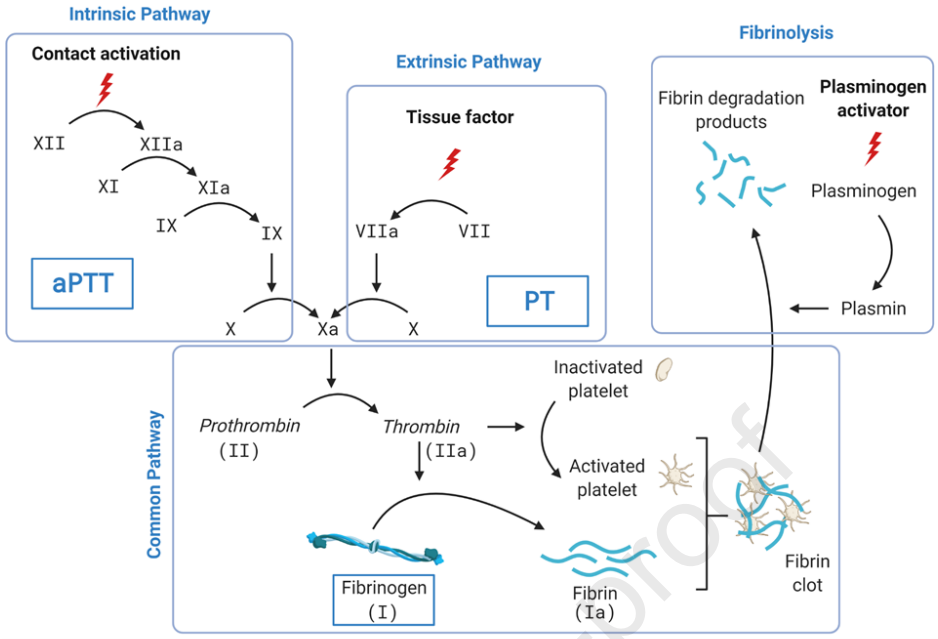

Figure 2

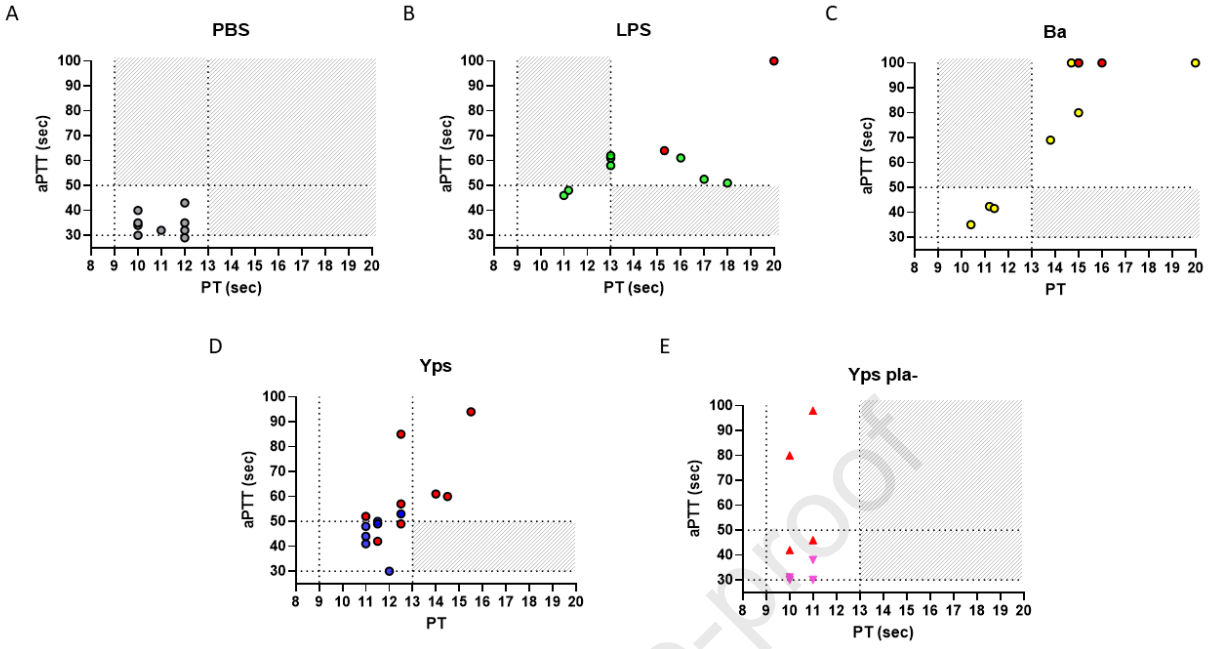

Figure 3

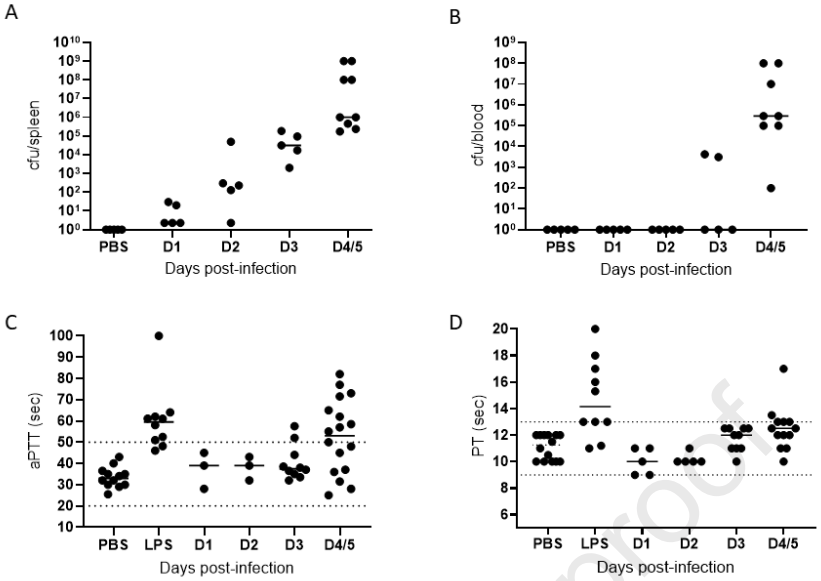

Figure captions

Fig.1 Schematic representation of human hemostasis cascades. The coagulation cascade starts either through the extrinsic pathway with the release of Tissue Factor after a trauma, or through the intrinsic pathway with activation of Factor XII by sub-endothelial extracellular matrix proteins such as collagen. Both pathways converge to the common pathway with the activation of Factor X that activates thrombin, which provokes the formation of fibrin clots. Clots of fibrin are degraded by plasmin during the fibrinolysis process. PT and aPTT tests allow to measure the time of coagulation for each pathway. Fibrinogen dosage give an estimation of the consumption of circulating fibrinogen, hence an estimation of formation of fibrin clots.

Fig.2: Plotting of Activated partial thromboplastin time versus Prothrombin time in treated-mice.

Groups of mice received: 100 uL of PBS subcutaneously (**A**), 100 uL of various concentrations of LPS intraperitoneally (**B**), 10^6 spores of *B. anthracis ΔpagA 9602P* subcutaneously (**C**), $1.5x10^3$ cfu of *Y. pestis* CO92 subcutaneously (**D**), or $2x10^6$ cfu of *Y. pestis ΔpPla* subcutaneously (**E**). Mice were sacrificed 24-36h after injection (or 16h for LPS), and plasmatic aPTT and PT were measured. Dotted lines represent the normal value thresholds: 9s<PT<13s, and 30s<aPTT<50s. Each dot represents an individual mouse. Moribund animals are identified with red color. Actual values, bacterial enumeration, and animal status are indicated in Table 1.

Fig.2 Bacterial load, aPPT and PT kinetics in *Y. pestis*-infected mice.

Groups of mice infected subcutaneously with 100 cfu of *Y. pestis* CO92 were sacrificed every 24h for 5 days and their blood and spleen were taken. Pooled data from groups of mice that received PBS and were sacrificed in parallel over 5 days served as negative controls (**A-D**).

Data from LPS-challenged mice from Table 1 are indicative of aPTT and PT values of LPS-induced DIC (**C** and **D**). Bacterial loads were quantified in spleen (**A**) and blood (**B**). Plasmatic aPTT (**C**) and PT (**D**) were measured every day. Since some mice were already moribund on D4, the data from D4 and D5 were pooled. Horizontal dotted lines represent the normal value thresholds. Short horizontal black bars represent the median. Some missing data for aPTT on D1 and D2 are due to an insufficient amount of blood collected to perform all measurements.